Original Article

JCBFM

Journal of Cerebral Blood Flow & Metabolism
0(0) 1–14

DOI: 10.1177/0271678X20910302
journals.sagepub.com/home/jcbfm
SAGE

Assessment of vascular stiffness in the internal carotid artery proximal to the carotid canal in Alzheimer's disease using pulse wave velocity from low rank reconstructed 4D flow MRI

Leonardo A Rivera-Rivera[1], Karly A Cody[2], Laura Eisenmenger[3], Paul Cary[2], Howard A Rowley[2,3], Cynthia M Carlsson[2,4], Sterling C Johnson[2,4] and Kevin M Johnson[1,3]

Abstract

Clinical evidence shows vascular factors may co-occur and complicate the expression of Alzheimer's disease (AD); yet, the pathologic mechanisms and involvement of different compartments of the vascular network are not well understood. Diseases such as arteriosclerosis diminish vascular compliance and will lead to arterial stiffness, a well-established risk factor for cardiovascular morbidity. Arterial stiffness can be assessed using pulse wave velocity (PWV); however, this is usually done from carotid-to-femoral artery ratios. To probe the brain vasculature, intracranial PWV measures would be ideal. In this study, high temporal resolution 4D flow MRI was used to assess transcranial PWV in 160 subjects including AD, mild cognitive impairment (MCI), healthy controls, and healthy subjects with apolipoprotein ε4 positivity (APOE4+) and parental history of AD dementia (FH+). High temporal resolution imaging was achieved by high temporal binning of retrospectively gated data using a local-low rank approach. Significantly higher transcranial PWV in AD dementia and MCI subjects was found when compared to old-age-matched controls (AD vs. old-age-matched controls: $P<0.001$, AD vs. MCI: $P=0.029$, MCI vs. old-age-matched controls $P=0.013$). Furthermore, vascular changes were found in clinically healthy middle-age adults with APOE4+ and FH+ indicating significantly higher transcranial PWV compared to controls ($P<0.001$).

Keywords

4D flow MRI, Alzheimer's disease, arterial stiffness, hemodynamics, PWV

Received 20 August 2019; Revised 27 January 2020; Accepted 7 February 2020

Introduction

Cerebrovascular disease (CVD) and Alzheimer's disease (AD) have traditionally been considered independent but potentially co-occurring pathways to dementia; however, pathology burden from both diseases is frequently found in the aging brain,[1,2] and both share common risk factors including APOE4 alleles, hypertension, diabetes mellitus, and age.[3,4] It remains unclear and controversial whether CVD precedes or follows AD and whether effects are additive or synergistic in driving cognitive decline. There is a prevailing

[1]Department of Medical Physics, University of Wisconsin School of Medicine and Public Health, Madison, WI, USA
[2]Alzheimer's Disease Research Center, University of Wisconsin School of Medicine and Public Health, Madison, WI, USA
[3]Department of Radiology, University of Wisconsin School of Medicine and Public Health, Madison, WI, USA
[4]Geriatric Research Education and Clinical Center, William S. Middleton Memorial Veterans Hospital, Madison, WI, USA

Corresponding author:
Kevin M Johnson, Wisconsin Institute for Medical Research, University of Wisconsin-Madison, Rm 1133, 1111 Highland Ave, Madison, WI 53705-2275, USA.
Email: kmjohnson3@wisc.edu

hypothesis that vascular dysfunction is a prominent and early feature in prodromal AD either as a concomitant or intrinsic feature.[5] A variety of magnetic resonance imaging (MRI)-based techniques are capable of probing vascular disease including T2-weighted-fluid-attenuated inversion recovery (T2FLAIR) for white matter hyperintensities assessment, dynamic contrast enhanced (DCE) for blood–brain barrier permeability, and arterial spin labeling (ASL) for tissue perfusion.[6–8]

An emerging technique that holds potential to provide multiple biomarkers of vascular health is 4D flow MRI. 4D flow MRI allows whole brain coverage and the quantification of blood velocities in most of the brain's feeding arteries or draining veins, making it well suited for cerebrovascular hemodynamic assessment.[9,10] Furthermore, previous studies using 4D flow found statistically significant reduced blood flow and increased pulsatility index (PI) in AD subjects compared to controls.[11–13] 4D flow also has the potential ability to measure pulse wave velocity (PWV), the speed of the cardiac pulse pressure along the arteries. PWV from 4D flow MRI has been validated in vitro and in vivo in the aorta, producing reliable and reproducible estimates.[14,15] PWV is currently the gold standard non-invasive biomarker of arterial stiffness, a significant risk factor for cardiovascular disease and mortality.[16] Typically measured from carotid-to-femoral artery ratios (cfPWV) using applanation tonometry,[16] PWV characterizes vascular compliance. Recent studies have found significant associations with progressive deposition of amyloid beta (Aβ) (a biomarker for AD) and arterial stiffness by measures of global PWV in nondemented individuals.[17,18]

A limitation of both cfPWV using applanation tonometry and aortic PWV using 4D flow is that these approaches do not directly probe cranial arteries. Experimental evidence indicates that arterial properties are heterogeneous and the vessel wall experiences different stimuli at different locations along the vascular system, which can lead to different phenotypes.[19,20] Therefore, methods to directly probe PWV in smaller arteries, such as intracranial arteries, are desirable. Transcranial Doppler ultrasound (TCD) can be used to derive intracranial PWV measures[21]; however, using TCD can be challenging due to measurement sensitivity to the direction of the blood flow with respect to the probe and operator dependence. Furthermore, the distance traveled by the pulse wave is highly challenging to assess accurately with the limited acoustic window of the arterial probe. A previous 2D phase contrast (PC) MRI study estimated PWV at the neck level in the common carotid arteries.[22] This study suggested high temporal resolution (e.g. $<$15 ms) is necessary for transcranial PWV estimates. More recently, a group of researchers demonstrated a method to attain high temporal resolution with 2D PC MRI and also estimated PWV at the neck level in the common carotid arteries.[23] In their study, high temporal binning of retrospectively gated data was achieved using a compress sensing (CS) reconstruction approach reaching a temporal resolution of 4 ms. This approach seems promising; however, assessment of the intracranial vasculature using 2D methods can be time consuming because each vessel segment requires another 2D scan prescribed orthogonal to the local vessel orientation. Furthermore, each slice is acquired at a different ensemble of heart beats, which can introduce undesirable and potentially confounding variability.

4D flow MRI is well suited to probe the tortuous vascular territories of the cerebrovasculature during one ensemble of heart beats. 4D flow provides accurate measures of flow values[24] with good agreement with flow probes[25] and measurement in model systems.[26] 4D flow indices are also highly correlated with those from TCD, although those from MRI are underestimated by approximatively 30%[27]; however, similar to with 2D, PWV measurements will require high temporal resolution to capture the pulse wave propagation along the arteries. Previous studies have estimated intracranial pulse wave transit time using 4D flow, finding significantly shorter transit times of the pulse wave from arteries to veins in AD subjects compared to cognitively healthy age-matched subjects. Unfortunately, intracranial PWV measurements were limited by temporal resolution.[12] Acquiring both high temporal and spatial resolution brain images to probe small arteries using 4D flow MRI is challenging because it typically requires long scan times (e.g. $\gg$10 min). Recent advances in constrained image reconstruction, as demonstrated in 2D PC MRI,[23] hold promise to allow for increased temporal resolution while maintaining sufficient spatial resolution (e.g. $<$2 mm). For example, in breast lesion assessment with 3D radial DCE MRI,[28] local low-rank (LLR) reconstruction approaches have been used to successfully increase the achievable temporal resolution. LLR methods enforce sparsity in space and time by promoting low rank of spatially decomposed overlapping blocks[29] and should be well suited for 4D flow of the intracranial vasculature.

In this study, we used retrospective high temporal binning of radial 4D flow data combined with LLR reconstruction to increase the achievable temporal resolution. In addition, the temporal resolution limit of 4D flow MRI was increased by assigning single flow encodes to the temporal bins during reconstruction. Subsequently, the achieved temporal resolution was exploited to assess cerebrovascular stiffness by means of PWV in the transcranial arteries of AD and MCI subjects as well as in healthy subjects with apolipoprotein ε4 positivity (APOE4+) and parental history of

AD dementia (FH+). To our knowledge, this is the first 4D flow MRI study that explores high temporal resolution imaging to estimate transcranial PWV in AD subjects. We hypothesized that high temporal resolution 4D flow MRI allows quantitation of PWV in the transcranial arteries. Furthermore, we hypothesized that AD subjects will have higher PWV compared to age-matched controls.

Materials and methods

Subjects and clinical classification

A total of 160 (mean age = 68 ± 10 years) participants from the Wisconsin Alzheimer's Disease Research Center (WADRC) and Wisconsin Registry for Alzheimer's Prevention (WRAP)[30] were analyzed for this study. The study population included cognitively healthy middle-aged adults, cognitively healthy older adults, MCI, and AD dementia clinical syndrome subjects. The middle-aged (age 45 to 65 years) subjects were stratified into two groups, controls and APOE4+, FH+, due absence or presence of both APOE4 allele and parental family history of AD dementia. All of these individuals were diagnostically characterized in the Wisconsin ADRC's multidisciplinary consensus conferences using applicable clinical, laboratory, and imaging criteria.[31–35] The University of Wisconsin Institutional Review Board approved all study procedures and protocols following the policies and guidance established by the campus Human Research Protection Program (HRPP). Each participant provided signed written informed consent before participation. Additional demographic data can be found in Table 1.

Subjects in the present study are part of the large National Alzheimer's Coordinating Center's (NACC) Uniform Dataset. Subjects given a consensus diagnosis of a non-Alzheimer's variant of dementia (e.g. Frontotemporal Dementia, Lewy Body Dementia, or Vascular Dementia) were excluded from this study. Cognitive assessment was performed as described in previous work,[13] and all MRI scans were reviewed by a neuroradiologist (H.A. Rowley) for incidental findings.

The present study consists of data from 160 newly recruited subjects. The number of subjects in this study was determined by the inclusion criteria consisting of: having a diagnosis of AD dementia clinical syndrome at the time of the 4D flow MRI scan, diagnosis of MCI attributed to AD at the time of the scan, cognitively unimpaired older adults, middle-age cognitively unimpaired who were APOE4+, FH+, and middle-age cognitively unimpaired who were APOE4−, FH−. Besides these criteria, having a high quality 4D flow MRI acquisition (e.g. projections >10,000, 32-channel head coil) with usable cardiac triggers was required. A scan with usable cardiac triggers was defined as having >90% of cardiac trigger values within the expected R-R interval. The expected R-R interval was determined from the median of all data. Exclusion criteria overseen by the clinical supervising physician (C. M. Carlsson) included stroke or other significant medical conditions such as major systemic illness or cancer.

Imaging protocol

Volumetric, time-resolved 3D PC MRI data with 5-point balanced flow encoding[36] were acquired on a 3.0 T system (MR750, GE Healthcare) using a 3D radially undersampled sequence[37,38] from July 2015 through November 2018. The study protocol used a

Table 1. Demographic information.

	Total ($n = 160$)	AD ($n = 28$)	MCI ($n = 34$)	Older cognitively healthy ($n = 42$)	Middle-age APOE4+, FH+ ($n = 24$)	Middle-age APOE4−, FH− ($n = 32$)
Age (years)	68 ± 10	72 ± 10	73 ± 9	73 ± 7	59 ± 3	58 ± 5
Female (*n*, %)	100, 63	17, 61	17, 50	25, 60	17, 71	24, 75
Parental dementia history positive (*n*, %)	54, 34	11, 39	18, 53	2, 5	24, 100	0, 0
APOE ε4 carrier (*n*, %)*	45, 28	10, 36	10, 29	1, 2	24, 100	0, 0
SBP (mmHg)	128 ± 18	131 ± 20	131 ± 17	132 ± 21	122 ± 10	122 ± 14
DBP (mmHg)	77 ± 8	74 ± 8	77 ± 6	77 ± 9	77 ± 7	79 ± 7
HR (bpm)	60 ± 9	59 ± 10	57 ± 12	61 ± 9	61 ± 7	59 ± 10
CHS scores	2.4 ± 1.8	3.4 ± 2.4	2.9 ± 1.9	2.6 ± 1.6	1.4 ± 0.6	1.6 ± 1.0

AD: Alzheimer's disease; APOE: apolipoprotein E; DBP: diastolic blood pressure; HR: heart rate; MCI: mild cognitive impairment; SBP: systolic blood pressure; CHS: cardiovascular Health Study.

*Nineteen subjects not genotyped (seven AD, nine MCI, three middle-age APOE4-, FH-); carrier refers to presence of at least one APOE E4 allele.

32-channel head coil (Nova Medical, Wilmington, MA). Data were acquired with the following imaging parameters Venc = 80 cm/s, imaging volume = $22 \times 22 \times 10$ cm^3, TR/TE = 7.4/2.7 ms, scan time ~7 min, acquired spatial resolution = 0.7 mm isotropic, flip angle = 8°, bandwidth = 250 kHz, number of projections ~11,000. For each subject, cardiac triggers were collected from a photoplethysmogram on a pulse oximeter worn on the subject's finger during the exam to be used for retrospective image reconstruction. 3D T2-weighted fluid-attenuated inversion recovery (FLAIR) images were acquired using TI = 1868 ms, TR = 6000 ms, TE = 123 ms, flip angle = 90°, FOV = 25.6×25.6 cm^2, slice thickness = 2.0 mm and spatial resolution = $1 \times 1 \times 2$ mm^3. T2FLAIR images were evaluated by two neuroradiologists (H.R., L. E.) blinded to clinical variables. White matter hyperintensity (WMH) burden was quantified from T2FLAIR images using the Cardiovascular Health Study (CHS) scale, where a "0" represents no evidence of WMH lesion and a "9" reflects involvement of all white matter.[39,40]

LLR 4D flow reconstruction and interleaved flow encode split

Flow-encoded images were retrospectively reconstructed using iterative SENSE[41] with ESPIRiT[42] sensitivity maps and a LLR constraint.[23,28,29,41,42] This reconstruction enforces a local temporal constraint using a nuclear norm minimization. Reconstructions were performed with block shifting of a $4 \times 4 \times 4$ block and an empirically tuned regularization parameter ($\lambda = 0.01$).

Typically, during a retrospectively gated 3D radial 4D flow acquisition, data are acquired with interleaved flow encoding to achieve uniform sampling of k-space in all encodes. At least four encodes are acquired to solve for velocities in x, y, and z directions and to remove background field offsets. In this study, we used five encodes to improve signal-to-noise ratio (SNR) of velocity images.[36] During traditional SENSE reconstruction, velocity maps for x, y and z are generated for each cardiac frame by averaging velocity encodes from same projection angles. This approach enforces data for velocity maps and the reference encode (for background field subtraction) to have same projection angle and minimizes residual artifacts in the velocity maps after background field subtraction. One limitation of this approach is that sets a theoretical temporal resolution limit equal to the # of encodes times the TR. In this study, a 5-point balanced encoding approach was used for a temporal resolution limit of 5 TRs (~37 ms). We used a LLR reconstruction, which is substantially less sensitive to the sampling pattern, to split the velocity encodes and assign them independently to cardiac frames. By assigning single encodes to cardiac frames during reconstruction, the theoretical temporal resolution limit was reduced to less than 1TR (e.g. 7.4 ms) instead of 5 TRs. Therefore, the LLR reconstruction approach was used to enable the acceleration inherent with the higher temporal resolution binning. Data were LLR reconstructed into 100 cardiac time frames using vendor-supplied detected gate positions from a pulse oximeter. To increase temporal resolution, spatial resolution was traded off and images were reconstructed to an isotropic spatial resolution of 1.7 mm. The high temporal resolution LLR images were compared with traditional SENSE images that were reconstructed into 20 cardiac time frames and 0.7 mm isotropic spatial resolution.

PWV analysis

Temporal reconstruction of the cardiac cycle was data limited to 100 time frames with current protocol. To avoid discretization errors, flow waveforms were interpolated to 500 points using splines.[15] Based on spatial resolution limits (1.7 mm isotropic), vessels with diameters larger than 3.4 mm were accessible for analysis. Previous studies showed the cervical and petrous segments of the internal carotid artery (ICA) have vessel diameters larger than the 3.4 mm limit.[13,43] Therefore, spatial distance and temporal shifts between cardiac waveforms were determined at two distinct anatomical locations (bilaterally): the cervical aspect of the ICA and the petrous aspect of the ICA (Figure 1). Cardiac waveform extraction and Euclidean distance calculations were performed in a customized MATLAB-based tool (Mathworks, Natick, MA) on the dynamic data.[44] This approach extracts the vascular tree using a centerline process with local cross-sectional cut-planes automatically placed in every centerline point perpendicular to the axial direction of the vessel. Time-averaged regions of interest (ROIs) were automatically contoured using a k-means clustering approach under the assumption that any cross section will contain a low-signal background and a vessel region. The distance between measurement planes was calculated along the vessel path using the centerline coordinates in space. The temporal shifts between cardiac waveforms were estimated from differences in the time-to-upstroke (TTU), which is the point of maximum acceleration on the upstroke of the waveform. Prior 4D flow MRI studies have shown TTU to be a reliable algorithm that produces PWV estimates similar in magnitude and variability to those found in the literature.[15] PWV was defined as the vessel length between measured waveform locations over their temporal shift.

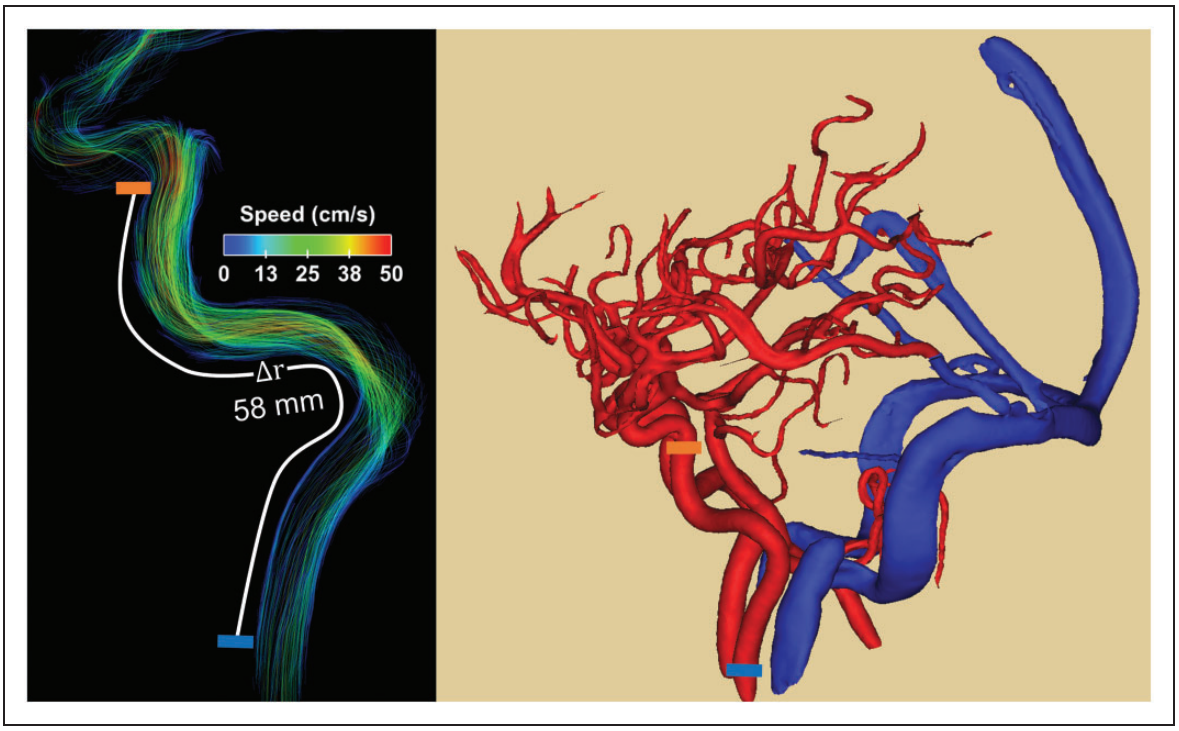

Figure 1. Example of blood flow velocity data (left) and high spatial resolution angiogram (right) derived from 4D flow MRI images. Pulse wave velocity (PWV) was estimated from time-resolved cardiac waveforms located at the cervical aspect of the internal carotid arteries (ICAs) (left, blue block) and petrous aspect of the ICA (left, orange block). The temporal shifts were derived from differences in the time to upstroke and the spatial distance from centerline coordinates along the vessel length.

Left and right ICA PWV estimates were averaged. Data analysis was performed blinded to subjects' clinical diagnosis (L.A. Rivera-Rivera). To compare LRR with traditional SENSE reconstruction, PWV was derived in a sample of AD subjects ($n = 25$) and older controls ($n = 25$).

Other 4D flow MRI-based markers: Blood flow and PI

Typical markers derivable from 4D flow images such as blood flow rates and PI were measured; however, the reconstruction scheme to achieve high temporal resolution 4D flow images reduces the spatial resolution and is suboptimal for deriving blood flow and PI measures (e.g. where high temporal resolution is not essential). Therefore, images were also reconstructed using the standard reconstruction. As previously described,[12] these images were reconstructed using SENSE, flow encodes were not split, spatial resolution was 0.7 mm isotropic, and 20 cardiac phases were retrospectively generated.

Blood flow and PI measures in the petrous aspect of the ICA were derived from cardiac waveforms extracted from three consecutive planes using 4D flow images. PI can be interpreted as a surrogate of distal cerebrovascular resistance.[45] In this study, PI was derived from velocity measurements in order to probe different velocity components, using two techniques. Flow PI was derived using the formula $(Q_{max} - Q_{min})/Q_{mean}$, where Q_{max}, Q_{min}, and Q_{mean} are the temporal max, min, and mean blood flow. A time-averaged vessel cross section was used. As a more segmentation insensitive measure, we also derived velocity PI, the pulsatility index of the peak velocity over the vessel mask, using the formula: $(V_{peak\text{-}max} - V_{peak\text{-}min})/V_{peak\text{-}mean}$. Where V_{peak} is a time-resolved quantity and is the maximum velocity enclosed in the vessel mask. This closely corresponds to the peak velocity measure that might be derived from ultrasound. It is less sensitive to the vessel mask but may be affected by time-dependent changes in the flow profile.

Statistical analysis

PWV, blood flow, and PI measurements were compared between groups. Furthermore, heart-rates (HR), systolic (SBP), and diastolic (DBP) blood pressure differences were evaluated between AD, MCI, and old-age-matched controls as well as between middle-age APOE4+, FH+ and middle-age-matched controls. The differences in these measurements were assessed

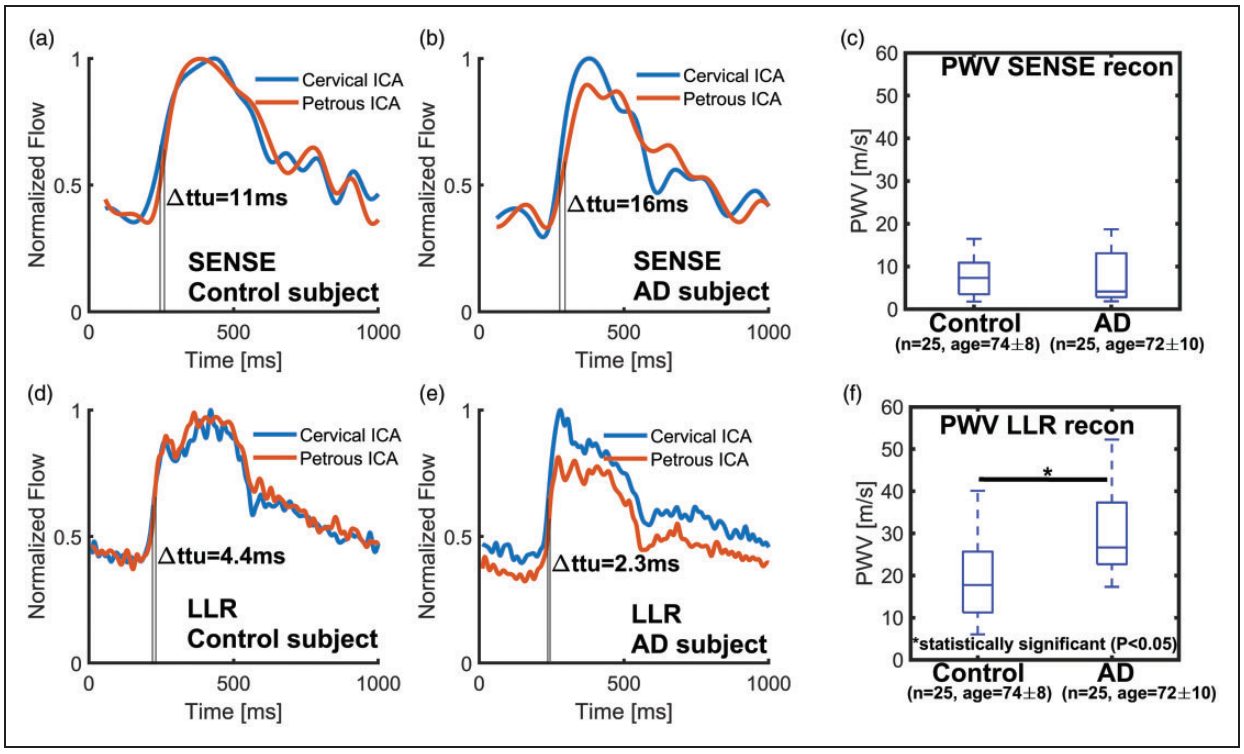

Figure 2. Flow curve examples from a healthy control (65 years old, female) and an Alzheimer's disease (AD) subject (63 years old, male) using traditional SENSE (a, b) and a local-low rank (LLR) (d, e) reconstruction. The time-to-upstroke differences (Δttu) between petrous and cervical internal carotid arteries (ICAs) flow curves were 11 ms using SENSE and 4.4 ms using LLR for the healthy volunteer, while Δttu were 16 ms using SENSE and 2.3 ms using LLR for the AD subject. For the healthy control, pulse wave velocity (PWV) was 4.1 m/s with SENSE and 10 m/s with LLR, while for the AD subject, PWV was 2.5 m/s with SENSE and 18 m/s with LLR. PWV was measured in a sample of age-matched controls and AD subjects from 4D flow images reconstructed using SENSE (c) to 20 cardiac frames and using local low-rank (LLR) (f) to 100 cardiac frames. No significant differences ($P > 0.05$) were detectable between PWV of controls and AD subjects when using the low temporal resolution SENSE reconstruction; however, a statistically higher PWV ($P = 0.001$) was measured in AD subjects compared to controls when using the high temporal resolution LLR approach.

using ANOVA followed by post hoc analysis using the Tukey–Kramer method. Statistical analysis was performed in MATLAB. $P < 0.05$ was set as the threshold for statistical significance.

Results

Based on each subject's heart rate (mean: 60 ± 9 bpm), the average temporal resolution derived from all datasets was 9.5 ± 1.5 ms. The average vessel length between measured waveforms and the flow waveform temporal shifts were 57 ± 16 mm and 4.8 ± 3.4 ms, respectively. In this study cohort, no significant differences ($P > 0.05$) between SBP, DBP, and HR were found between AD, MCI, and older controls or between middle-age APOE4+, FH+ and middle-age controls (e.g. APOE4−, FH−). WMH burden CHS scores were largest in the AD group (CHS = 3.4 ± 2.4) (Table 1), but differences were not significant when compared to MCI and old-age-matched controls (AD vs. MCI $P = 0.586$; AD vs. old-age-matched controls $P = 0.169$; old-age-matched controls vs. MCI $P = 0.686$). No significant differences in CHS scores were found between middle-age controls and middle-age APOE4+, FH+ ($P = 0.305$).

Flow curves examples and PWV comparisons derived in a sample of AD subjects ($n = 25$) and age-matched controls ($n = 25$) using LLR and traditional SENSE reconstructions are summarized in Figure 2. Transcranial PWV was similar between both groups when using traditional SENSE ($P = 0.614$) (Figure 2 (c)), but when using LLR (Figure 2(f)), a statistically higher transcranial PWV was measured in AD compared to older controls ($P = 0.001$).

PWV and age

Measurements of transcranial PWV in AD, MCI, and older controls are summarized in Figure 3(a). The average transcranial PWV of the AD group (median: 26.5 $\pm$ 8.5 m/s) was the highest among the groups with differences reaching statistical significance when

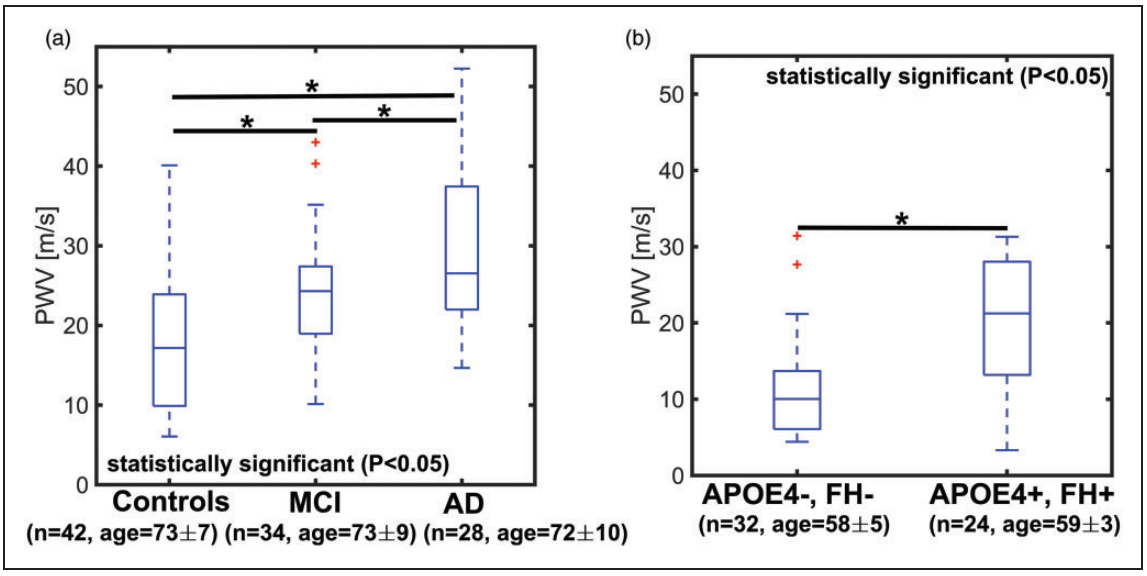

Figure 3. Boxplots of transcranial pulse wave velocity (PWV) in older controls, mild cognitively impaired (MCI), and Alzheimer's disease (AD) subjects (a) and middle-age APOE4+, FH+ and controls (e.g. APOE4−, FH−) (b). PWV was estimated from high temporal resolution images derived using a local low-rank (LLR) reconstruction. A statistically higher transcranial PWV was measured in AD ($P < 0.001$) and MCI ($P = 0.013$) subjects when compared to age-matched controls. The MCI group appeared to be in transition towards higher transcranial PWV, while AD subjects showed the highest transcranial PWV in this cohort. MCI and AD transcranial PWV were also significantly different ($P = 0.029$). A statistically higher transcranial PWV ($P < 0.001$) was measured in middle-age APOE4+, FH+ when compared to middle-aged control adults (APOE4−, FH−), suggesting early vascular changes in subjects with APOE4+, FH+.

compared to old-age-matched controls (median: 17.2 ± 7.4 m/s) and MCI subjects (median: 24.3 ± 5.7 m/s) (AD vs. old-age-matched controls: $P < 0.001$; AD vs. MCI: $P = 0.029$). Differences between the MCI group and controls were also significant (MCI vs. old-age-matched controls $P = 0.013$). Comparison between middle-age-matched controls and middle-age APOE4+, FH+ are shown in Figure 3(b). Overall, middle-age APOE4+, FH+ subjects recorded an elevated transcranial PWV (median: 21.2 ± 7.5 m/s) when compared to middle-age-matched controls (median: 10.0 ± 4.8 m/s). Differences between groups were significant ($P < 0.001$).

Linear regression models are shown in Figure 4. A higher transcranial PWV is appreciable in both AD (a) and MCI (b) subjects for all ages with a weak response to increasing age (AD: $R^2 = 0.017$, MCI: $R^2 = 0.009$). In controls (c), transcranial PWV shows a stronger correlation with age ($R^2 = 0.305$). In the middle-age APOE4+, FH+ group, transcranial PWV (d) is higher than for control adults in the same age range and responds weakly to increasing age ($R^2 = 0.001$).

Blood flow and pulsatility index

Mean velocity curves used to derive blood flow measurements for each subgroup are available as supplementary material (Supplementary Figure 1). Blood flow in the ICAs was significantly lower in AD when compared to age-matched controls (Figure 5(a)) (AD vs. old-age-matched controls: $P = 0.046$, AD vs. MCI: $P = 0.059$, MCI vs. age-matched controls: $P = 0.999$). In the APOE4+, FH+ group, ICA blood flow was 237 ± 34 mL/min and 217 ± 32 mL/min in middle-age-matched controls (Figure 5(b)) ($P = 0.076$). Velocity PI in AD and MCI subjects was statistically larger than in older controls (Figure 6(a)) (AD vs. age-matched controls: $P = 0.003$, MCI vs. age-matched controls: $P = 0.046$, AD vs. MCI: $P = 0.550$). While flow PI measurements were higher in AD, this was only found to be statistically significant when compared to age-matched controls (Figure 6(c)) (AD vs. age-matched controls: $P = 0.041$, MCI vs. age-matched controls: $P = 0.149$, AD vs. MCI: $P = 0.792$). The velocity and flow PI between APOE4+, FH+ and middle-aged-matched controls were similar (velocity PI $P = 0.977$, flow PI $P = 0.771$) (Figure 6(b) and (d)).

Discussion

This study evaluated transcranial PWV in AD and MCI subjects, controls, and cognitively healthy subjects with APOE4+ and FH+ using high temporal resolution 4D flow MRI. High temporal resolution 4D

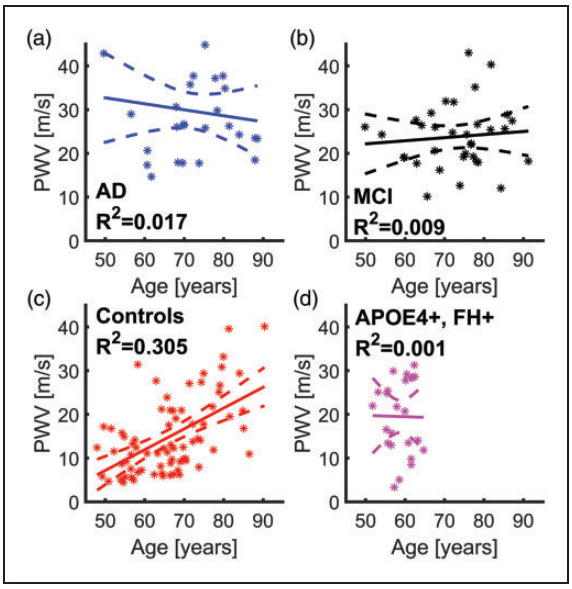

Figure 4. Scatter plots and linear regressions with 95% confidence intervals of transcranial pulse wave velocity (PWV) and age are shown for Alzheimer's disease (AD) subjects (a), mild cognitively impaired (MCI) subjects (b), healthy controls (c), and healthy subjects with APOE4+, FH+ (d). Transcranial PWV was highest in AD subjects for all ages and displayed a slow decrease with age in AD ($R^2 = 0.017$). For MCI subjects, transcranial PWV increased slightly with age ($R^2 = 0.009$); however, for controls, transcranial PWV increased in a more linear fashion ($R^2 = 0.305$). The middle-aged APOE4+, FH+ group (d) shows higher transcranial PWV compared to controls with similar age range ($R^2 = 0.001$).

flow imaging was achieved using a retrospectively reconstructed LLR approach combined with flow encode splitting. Elevated PWV measures were found in AD and MCI subjects compared to age-matched controls. In addition, a higher PWV was observed in younger healthy subjects with APOE4+ and FH+ when compared to healthy subjects with APOE4− and FH−. Collectively, these results suggest clinical diagnosis is concomitant with vascular stiffening, as evident from higher PWV in AD and MCI subjects. Furthermore, early vascular changes appeared to manifest in a group of clinically healthy subjects with parental history of dementia due to AD and APOE4 genotype. Importantly, this is the first study that uses high temporal resolution 4D flow MRI to quantify transcranial PWV in AD subjects.

In this study, transcranial PWV was largest in AD subjects followed by MCI and age-matched controls. These results suggest macrovascular disease with arterial stiffening in the ICAs of AD subjects. The MCI group appears to be in transition towards higher transcranial PWV, suggesting a positive correlation between arterial stiffness and degree of cognitive impairment. Further, linear regression models showed that younger AD subjects displayed PWVs similar to those of older subjects from the control group. This finding suggests a clinical diagnosis of AD is associated with a similar vessel stiffness of older age. These results agree with studies that report increased arterial stiffness in subjects with dementia of the vascular and AD types.[46] They are also in line with other studies that used applanation tonometry to estimate cfPWV and heart-carotid PWV (hcPWV).[17,18] These researchers found greater

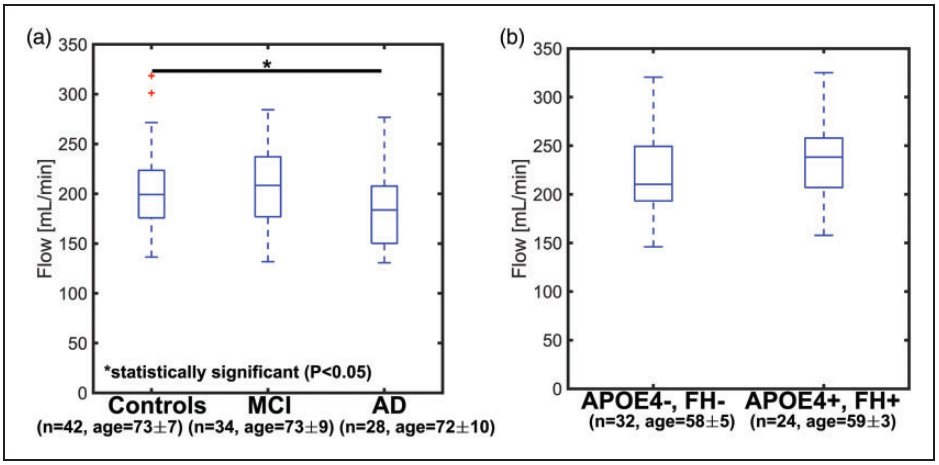

Figure 5. Boxplots showing ICA blood flow in older age-matched controls, mild cognitive impaired (MCI), and Alzheimer's disease (AD) subjects (a) and in middle-age APOE4+, FH+ and controls (APOE4−, FH−) (b). ICA blood flow was lowest in AD subjects with values of 206 ± 31 mL/min for older age-matched controls, 206 ± 33 for MCI, and 183 ± 29 for AD. ICA blood flow was significantly lower in AD when compared to older controls (AD vs. older controls: $P = 0.046$, AD vs. MCI: $P = 0.059$, MCI vs. older controls: $P = 0.999$). In the middle-aged control group, blood flow was 217 ± 32 mL/min, while flow was 237 ± 34 mL/min in the middle-aged APOE4+, FH+ group ($P = 0.076$).

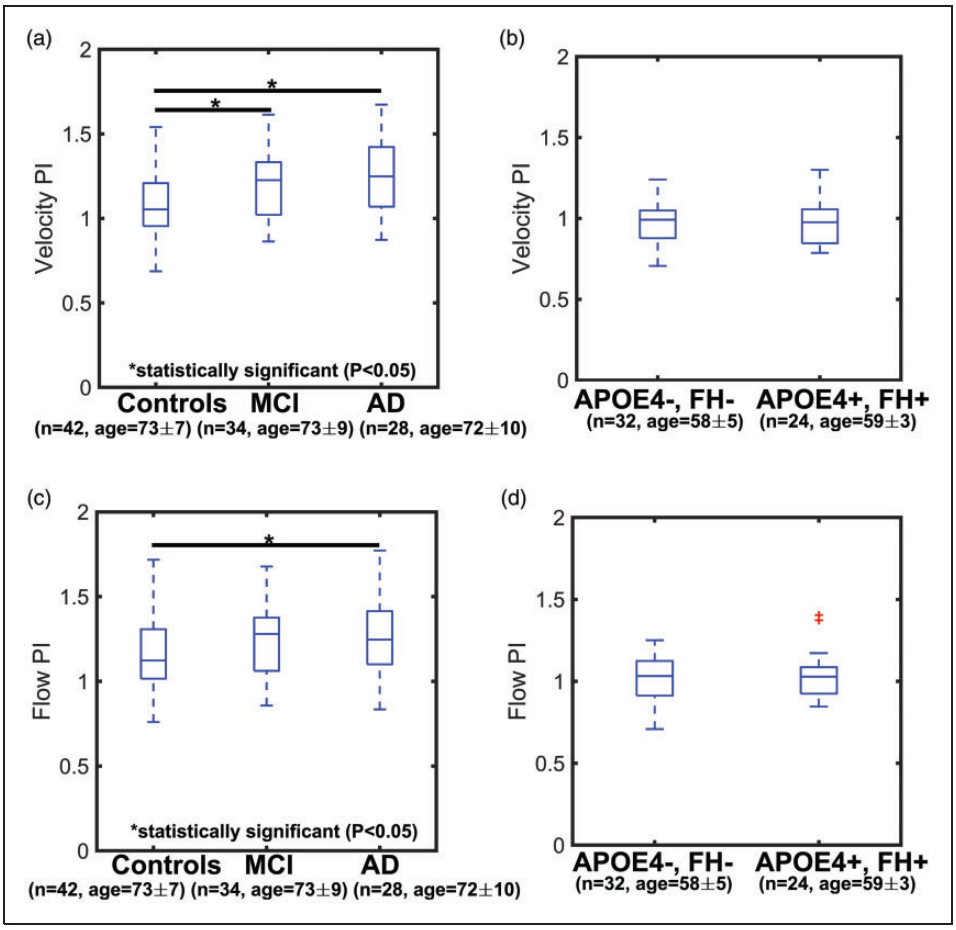

Figure 6. Boxplots showing velocity and flow pulsatility index (PI) in older controls, mild cognitive impaired (MCI), and Alzheimer's disease (AD) subjects (a, c) and in middle-aged adults with APOE4+, FH+ and age-matched controls (APOE4−, FH−) (b, d). A statistically higher velocity PI was measured in AD and MCI subjects when compared to age-matched controls with values of 1.08 ± 0.15 in older controls, 1.19 ± 0.16 in MCI, and 1.25 ± 0.19 in AD (AD vs. older controls: $P = 0.003$, AD vs. MCI: $P = 0.550$, MCI vs. older controls: $P = 0.046$). Flow PI measurements were 1.14 ± 0.17 in older controls, 1.24 ± 0.16 in MCI, and 1.27 ± 0.19 in AD (AD vs. older controls: $P = 0.041$, AD vs. MCI: $P = 0.792$, MCI vs. older controls: $P = 0.149$). Velocity and flow PI in the middle-aged control group and the APOE4+, FH+ group were similar: 0.97 ± 0.11 and 0.97 ± 0.10 (Velocity PI, $P = 0.977$) and 1.02 ± 0.12 and 1.03 ± 0.10 (Flow PI, $P = 0.771$), respectively.

arterial stiffness as measured by PWV to be associated with greater evidence of dementia-related brain parenchymal changes such as Aβ deposition, lower brain volumes, and high white matter hyperintensity burden. In this study, WMH burden was quantified from T2FLAIR images. CHS scores reflected a higher WMH burden in AD and MCI than in age-matched controls, although not significant (AD vs. MCI $P = 0.586$; AD vs. old-age-matched controls $P = 0.169$; old-age-matched controls vs. MCI $P = 0.686$). WMHs are not specific to cerebral vascular pathology alone and occur in other diseases and in normal aging,[47] suggesting limited ability to characterize specific CVD components.

Decreased arterial compliance (e.g. arterial stiffness) can lead to decreased dampening of the pressure pulse wave as it travels from arteries to brain tissue, ultimately depositing higher energy into the brain parenchyma. This altered energy deposition could lead to vascular and parenchymal injuries such as progression of cerebral small vessel disease (SVD) and increased Aβ deposition. Moreover, endothelial cells are sensitive to pulsatile wall shear stress. For example, through the phenomenon of mechanotransduction, endothelial cells can translate extracellular mechanical cues into intracellular biochemical signals, to regulate cellular maintenance of endothelial function.[20,48] Endothelial cells are crucial in the blood–brain barrier function, which can be compromised in patients with cerebrovascular disease.[49,50] 2D PC MRI studies have demonstrated higher pulsatility in cerebral perforating arteries is a marker of SVD.[51] While 4D flow MRI

studies have correlated higher pulsatility of intracranial arteries and veins with AD pathology.[11–13,52] Furthermore, vessel pulsatility has been speculated as a driver of glymphatic flow, as the motive force for perivascular drainage of interstitial fluid, Aβ, and other soluble metabolites.[53,54] Cardiac pulsations may also contribute to clearance of soluble metabolites from the brain by mixing and dispersion effects.[55,56] This mechanism can be diminished by the loss of arterial compliance, either by the normal process of aging or cerebrovascular disease. Subsequently, arterial stiffening would lead to a reduction in the amplitude of vasomotion.[57] This hypothesis suggests that microvascular pulsations are important for the removal of toxic solutes out of the brain; however, others argue that clearance of soluble metabolites from the brain happens through the intramural pariarterial drainage (IPAD) pathway.[58] The authors claim arterial pulsations are too weak to drive perivascular drainage. They suggest clearance of toxic metabolites is driven by contraction of vascular smooth muscle cells pushing fluids through the basement membranes in the walls of cerebral arteries. It is still unclear what mechanisms drive clearance of soluble metabolites from the brain and whether vascular pathology precedes, follows, or enhances AD pathology. Further research is essential to unravel this relationship.

Higher transcranial PWV was found in clinically healthy adults who all had APOE4 positivity and self-reported parental history of dementia due to AD. The APOE4 genotype is a genetic risk factor for both AD and cardiovascular disease[59]; however, APOE4 genotype itself is a relative poor indicator of AD risk, and effects are often only observed with reasonable significance in much larger cohorts. APOE is a lipid transport protein and major ligand for low density lipoprotein (LDL) receptors with functions related to cholesterol metabolism and cardiovascular disease. Interestingly, evidence strongly associates vascular midlife risk factors and cardiovascular genes with increased risk for AD and Aβ deposition.[4,60] These results suggest AD and vascular pathology might interact in a synergistic manner with combined effects equating to greater than the sum of their separate contributions; however, as mention previously, experiments designed specifically to address these questions and to discern the chronology of these pathologies are necessary.

Blood flow and PI in the ICAs were also assessed in this study, and results showed similar trends to those found previously.[13] Significantly lower blood flow rates were found in AD subjects when compared to controls. Velocity PI showed larger group differences than flow PI, meaning area measurements can potentially mask PI effects. PWV measures were statistically different among cohorts and *P*-values were smaller than for blood flow rates and PI measures, suggesting PWV might be a more sensitive marker of cerebrovascular health. Furthermore, decreased blood flow might not directly reflect vascular health and simply be a marker of decreased metabolism due to neuron death. PI might not be a direct marker of vascular health either, but rather a descriptor of a complex relationship between multiple hemodynamic variables (e.g. cerebrovascular resistance, cerebral perfusion pressure) as described by others.[45] As the gold standard measure for arterial stiffness, transcranial PWV could be the most appropriate marker for cerebrovascular health although larger, longitudinal studies are needed to confirm its utility. Interestingly, the middle-age APOE4+, FH+ group showed higher cerebral blood flow in the ICAs than middle-age-matched controls, perhaps as response to subtle brain changes. In a previous study, blood flow in the ICAs of a group of cognitively healthy subjects with FH+ was 259 ± 40 mL/min; in this study, ICA blood flow in the APOE4+, FH+ group was 237 ± 34 mL/min.[12] These results are comparable but somewhat different. A direct comparison is limited by differences in groups (no APOE4+ genotyping in former group) and receiver coil hardware used in the experiments (8ch vs. 32ch head coil); however, a recent ASL study found an increase in cerebral blood flow and Aβ burden in cognitively normal subjects over the age of 65.[61] The authors argue their findings were due to potential compensatory mechanisms that protects against pathology in the pre-clinical stages of AD. More studies on the relation between cerebral blood flow rates and Aβ burden in cognitively healthy subjects at risk of dementia due to AD are warranted to explore the validity of the compensatory mechanism hypothesis.

PWV assessment using high temporal resolution imaging (e.g. 4 ms) exploiting undersampling and constrained reconstructions (e.g. CS, LLR) has been previously demonstrated in the common carotid arteries with 2D PC MRI.[23] In this study, similar principles were applied and extended in order to achieve high temporal resolution in 4D flow images. 4D flow imaging has the advantage of encoding in all three spatial dimensions, allowing for retrospective selection of arbitrary planes. Although this comes with an increased demand for acceleration, the acceleration can also be distributed in three spatial directions and in time. In this study, we achieved a temporal resolution of 10 ms, which was further interpolated for analysis. Although this is slightly higher than in the 2D approach, the measurements come from a single ensemble of heart beats. Furthermore, in a sample of AD subjects and older controls, transcranial PWV was similar between both groups when using traditional SENSE

($P = 0.614$); however, a statistically higher transcranial PWV was measured in AD compared to older controls ($P = 0.001$) when using LLR, thereby demonstrating the capability of LLR with flow encode split to estimate transcranial PWV compared to traditional reconstruction methods. PWV measurements from other studies[23] that used a similar reconstruction technique to increase temporal resolution of 2D images found a PWV of 7.9 ± 2.4 m/s from common carotids to cervical internal carotid arteries in 10 healthy subjects (62 ± 10 years old). In our study, the middle-age control group (58 ± 5 years old) had a PWV of 10.0 ± 6.5 m/s from cervical to petrous internal carotid arteries, which is slightly larger but still in good agreement. In this study, we used a 3D method along the internal carotid artery where it is reasonable to expect PWV to increase as the pulse wave moves from the extra-cranial vasculature into the skull. Another study[21] used TCD to measure cerebral PWV from the common carotid arteries to the middle cerebral arteries; they found a PWV of 5.0 ± 0.8 m/s in 90 younger healthy adults (46 ± 12 years old). These values are lower than our middle age healthy controls, but the subjects were also younger. Furthermore, the distance traveled by the pulse wave was measured along the body surface, which can lead to uncertainties in the PWV measurements.

Our study has several limitations. First, the LLR images have a lower spatial resolution (e.g. 1.7 mm isotropic) compared to the standard approach used previously (e.g. 0.68 mm isotropic).[13] This lower spatial resolution limits the ability to measure blood flow, PI, and PWV in small arteries. For example, PWV measurements in the middle cerebral artery (MCA) were not feasible as velocity profiles were close to noise levels due to a combination of lower spatial resolution and heavy undersampling. This problem can potentially be addressed by increasing both temporal and spatial resolution through acquiring more data at the expense of longer scan times. Second, the LLR approach enforces low rank model fitting, which, in combination with the lower spatial resolution, can lead to loss of pulsation amplitude in the time-resolved images. Since PI is estimated from pulsatile data, this model is not ideal for PI measurements. Further, systematic assessment of measurement variance is warranted, and the LLR reconstruction has not been compared against more standardized measures from TCD or gold standard measures from invasive pressure probes. Third, temporal shifts used for PWV estimates can be influenced by mechanisms such as wave reflections which make the correspondence of the measured PWV to true pressure PWV unknown. Finally, the participants with MCI and dementia were not biomarker confirmed to be in the AD continuum. Similarly the middle-age healthy subjects, while APOE4 and family history positive, were also not biomarker confirmed to be in the AD continuum nor were the APOE4 negative and family history negative subjects confirmed to be in the AD biomarker negative. Further studies are in progress to more directly examine the temporal associations between PWV and amyloid and tau pathobiology.

Sub-TR temporal shifts in the transcranial pulse wave were detectable in subjects with AD clinical syndrome using 4D flow MRI combined with a LLR reconstruction approach. Results suggest arterial stiffening, macrovascular damage, and premature macrovascular aging in the ICAs of AD and MCI subjects. These findings add to mounting evidence that relates functional changes in the arterial system to AD and demonstrate the potential of vascular imaging biomarkers for the characterization of AD. Furthermore, early vascular changes were found in a group of cognitively normal, healthy subjects with APOE4+, FH+. The cognitive health of these subjects needs to be longitudinally assessed in order to address the questions whether CVD precedes or follows AD and whether effects are additive or synergistic in driving cognitive decline. Finally, as mentioned above, transcranial PWV measures need to be correlated with AD biomarkers such as brain atrophy, amyloid burden, and tau pathology.

Funding

The author(s) disclosed receipt of the following financial support for the research, authorship, and/or publication of this article: We gratefully acknowledge research support from GE Healthcare, and funding support from the Alzheimer's Association and NIH grants AARFD-20-678095, P50-AG033514, R01EB027087, R01NS066982, and R01AG021155.

Declaration of conflicting interests

The author(s) declared the following potential conflicts of interest with respect to the research, authorship, and/or publication of this article: SC Johnson served on an advisory board for Roche Diagnostics in 2018 for which he received an honorarium and is principal investigator of an equipment grant from Roche. He conducts tau imaging in NIH funded studies as well as a study funded by Cerveau Technologies using radioligand precursor material supplied by Cerveau Technologies.

Authors' contributions

1. Leonardo A Rivera-Rivera – Study design, MRI data reconstruction and post processing analysis, interpreting results, editing of the manuscript and figures

2. Karly A Cody – Assisted with study coordination of subjects, editing of the manuscript
3. Laura Eisenmenger – Imaging protocols, image quality insurance, editing of the manuscript and assessment of white matter hyperintensities
4. Paul Cary – Assisted with post processing analysis, editing of the manuscript
5. Howard A Rowley – Imaging protocols, image quality insurance, maintaining of the imaging archives and assessment white matter hyperintensities and brain morphology for co-morbid diseases
6. Cynthia M Carlsson – Clinical supervising physician for medical data collection, interpreting the results and editing of the manuscript
7. Sterling C Johnson – Study design, data acquisition, interpreting results and editing of the manuscript
8. Kevin M Johnson – Study design, MRI reconstruction optimization, interpreting results, editing of the manuscript

Supplementary material

Supplemental material for this article is available online.

References

1. Attems J and Jellinger KA. The overlap between vascular disease and Alzheimer's disease – lessons from pathology. *BMC Med* 2014; 12: 206.
2. Liu Y, Braidy N, Poljak A, et al. Cerebral small vessel disease and the risk of Alzheimer's disease: a systematic review. *Age Res Rev* 2018; 47: 41–48.
3. Casserly I and Topol EJ. Convergence of atherosclerosis and Alzheimer's disease: inflammation, cholesterol, and misfolded proteins. *Lancet* 2004; 363: 1139–1146.
4. Gottesman RF, Schneider ALC, Zhou Y, et al. Association between midlife vascular risk factors and estimated brain amyloid deposition. *JAMA* 2017; 317: 1443.
5. Sweeney MD, Montagne A, Sagare AP, et al. Vascular dysfunction – the disregarded partner of Alzheimer's disease. *Alzheimers Dement* 2019; 15: 158–167.
6. Wardlaw JM, Smith EE, Biessels GJ, et al. Neuroimaging standards for research into small vessel disease and its contribution to ageing and neurodegeneration. *Lancet Neurol* 2013; 12: 822–838.
7. Zwanenburg Jaco JM and van Osch Matthias JP. Targeting cerebral small vessel disease with MRI. *Stroke* 2017; 48: 3175–3182.
8. Vikner T, Nyberg L, Holmgren M, et al. Characterizing pulsatility in distal cerebral arteries using 4D flow MRI. *J Cereb Blood Flow Metab*, Epub ahead of print 13 November 2019. DOI: 10.1177/0271678X19886667
9. Markl M, Frydrychowicz A, Kozerke S, et al. 4D flow MRI. *J Magnet Reson Imag* 2012; 36: 1015–1036.
10. Wen B, Tian S, Cheng J, et al. Test–retest multisite reproducibility of neurovascular 4D flow MRI. *J Magnet Reson Imag* 2019; 49: 1543–1552.
11. Berman SE, Rivera-Rivera LA, Clark LR, et al. Intracranial arterial four-dimensional flow is associated with metrics of brain health and Alzheimer's disease. *Alzheimers Dement* 2015; 1: 420–428.
12. Rivera-Rivera LA, Schubert T, Turski P, et al. Changes in intracranial venous blood flow and pulsatility in Alzheimer's disease: a 4D flow MRI study. *J Cereb Blood Flow Metab* 2017; 37: 2149–2158.
13. Rivera-Rivera LA, Turski P, Johnson KM, et al. 4D flow MRI for intracranial hemodynamics assessment in Alzheimer's disease. *J Cereb Blood Flow Metab* 2016; 36: 1718–1730.
14. Ruesink T, Medero R, Rutkowski D, et al. In vitro validation of 4D flow MRI for local pulse wave velocity estimation. *Cardiovasc Eng Technol* 2018; 9: 674–687.
15. Wentland AL, Wieben O, François CJ, et al. Aortic pulse wave velocity measurements with undersampled 4D flow-sensitive MRI: comparison with 2D and algorithm determination. *J Magnet Reson Imag* 2013; 37: 853–859.
16. Laurent S, Cockcroft J, Van Bortel L, et al. Expert consensus document on arterial stiffness: methodological issues and clinical applications. *Eur Heart J* 2006; 27: 2588–2605.
17. Hughes TM, Wagenknecht LE, Craft S, et al. Arterial stiffness and dementia pathology: atherosclerosis risk in communities (ARIC)-PET study. *Neurology* 2018; 90: e1248–e1256.
18. Hughes TM, Kuller LH, Barinas-Mitchell EJM, et al. Arterial stiffness and β-amyloid progression in nondemented elderly adults. *JAMA Neurol* 2014; 71: 562.
19. Daemen Mat JAP and De Mey Jo GR. Regional heterogeneity of arterial structural changes. *Hypertension* 1995; 25: 464–473.
20. Dai G, Kaazempur-Mofrad MR, Natarajan S, et al. Distinct endothelial phenotypes evoked by arterial waveforms derived from atherosclerosis-susceptible and -resistant regions of human vasculature. *Proc Natl Acad Sci U S A* 2004; 101: 14871–14876.
21. Fu X, Huang C, Wong KS, et al. A new method for cerebral arterial stiffness by measuring pulse wave velocity using transcranial Doppler. *J Atheroscler Thromb* 2016; 23: 1004–1010.
22. Kröner ESJ, Lamb HJ, Siebelink H-MJ, et al. Pulse wave velocity and flow in the carotid artery versus the aortic arch: effects of aging: carotid artery pulse wave velocity. *J Magnet Reson Imag* 2014; 40: 287–293.
23. Peper ES, Strijkers GJ, Gazzola K, et al. Regional assessment of carotid artery pulse wave velocity using compressed sensing accelerated high temporal resolution 2D CINE phase contrast cardiovascular magnetic resonance. *J Cardiovasc Magnet Reson* 2018; 20: 86.
24. Dyverfeldt P, Bissell M, Barker AJ, et al. 4D flow cardiovascular magnetic resonance consensus statement. *J Cardiovasc Magn Reson* 2015; 17: 72–72.
25. Frydrychowicz A, Roldan-Alzate A, Winslow E, et al. Comparison of radial 4D Flow-MRI with perivascular ultrasound to quantify blood flow in the abdomen and introduction of a porcine model of pre-hepatic portal hypertension. *Eur Radiol* 2017; 27: 5316–5324.

26. Rutkowski DR, Reeder SB, Fernandez LA, et al. Surgical planning for living donor liver transplant using 4D flow MRI, computational fluid dynamics and in vitro experiments. *Comput Methods Biomech Biomed Eng Imaging Vis* 2018; 6: 545–555.
27. Chang W, Landgraf B, Johnson KM, et al. Velocity measurements in the middle cerebral arteries of healthy volunteers using 3D radial phase-contrast HYPRFlow: comparison with transcranial Doppler sonography and 2D phase-contrast MR imaging. *Am J Neuroradiol* 2011; 32: 57–59.
28. Jimenez JE, Strigel RM, Johnson KM, et al. Feasibility of high spatiotemporal resolution for an abbreviated 3D radial breast MRI protocol. *Magnet Reson Med* 2018; 80: 1452–1466.
29. Trzasko JD and Manduca A. Calibrationless parallel MRI using CLEAR. In: *2011 conference record of the forty fifth Asilomar conference on signals, systems and computers (ASILOMAR)*, Pacific Grove, CA, USA, 6–9 November 2011, pp.75–79. Piscataway, NJ: IEEE.
30. Johnson SC, Koscik RL, Jonaitis EM, et al. The Wisconsin Registry for Alzheimer's prevention: a review of findings and current directions. *Alzheimers Dement* 2017; 10: 130–142.
31. Jack CR, Bennett DA, Blennow K, et al. NIA-AA research framework: toward a biological definition of Alzheimer's disease. *Alzheimers Dement* 2018; 14: 535–562.
32. McKhann G, Drachman D, Folstein M, et al. Clinical diagnosis of Alzheimer's disease: report of the NINCDS-ADRDA Work Group* under the auspices of Department of Health and Human Services Task Force on Alzheimer's disease. *Neurology* 1984; 34: 939–944.
33. McKhann GM, Knopman DS, Chertkow H, et al. The diagnosis of dementia due to Alzheimer's disease: recommendations from the National Institute on Aging-Alzheimer's Association workgroups on diagnostic guidelines for Alzheimer's disease. *Alzheimers Dement* 2011; 7: 263–269.
34. Albert MS, DeKosky ST, Dickson D, et al. The diagnosis of mild cognitive impairment due to Alzheimer's disease: recommendations from the National Institute on Aging-Alzheimer's Association workgroups on diagnostic guidelines for Alzheimer's disease. *Alzheimers Dement* 2011; 7: 270–279.
35. Sperling RA, Aisen PS, Beckett LA, et al. Toward defining the preclinical stages of Alzheimer's disease: recommendations from the National Institute on Aging-Alzheimer's Association workgroups on diagnostic guidelines for Alzheimer's disease. *Alzheimers Dement* 2011; 7: 280–292.
36. Johnson KM, Markl M. Improved SNR in phase contrast velocimetry with five-point balanced flow encoding. *Magnet Reson Med* 2010; 63: 349–355.
37. Johnson KM, Lum DP, Turski PA, et al. Improved 3D phase contrast MRI with off-resonance corrected dual echo VIPR. *Magnet Reson Med* 2008; 60: 1329–1336.
38. Gu T, Korosec FR, Block WF, et al. PC VIPR: a high-speed 3D phase-contrast method for flow quantification and high-resolution angiography. *Am J Neuroradiol* 2005; 26: 743–749.
39. Manolio TA, Kronmal RA, Burke GL, et al. Magnetic resonance abnormalities and cardiovascular disease in older adults. The Cardiovascular Health Study. *Stroke* 1994; 25: 318–327.
40. Moghekar A, Kraut M, Elkins W, et al. Cerebral white matter disease is associated with Alzheimer pathology in a prospective cohort. *Alzheimers Dement* 2012; 8: S71–S77.
41. Pruessmann KP, Weiger M, Scheidegger MB, et al. SENSE: sensitivity encoding for fast MRI. *Magnet Reson Med* 1999; 42: 952–962.
42. Uecker M, Lai P, Murphy MJ, et al. ESPIRiT – an Eigenvalue approach to autocalibrating parallel MRI: where SENSE meets GRAPPA. *Magnet Reson Med* 2014; 71: 990–1001.
43. Krejza J, Arkuszewski M, Kasner SE, et al. Carotid artery diameter in men and women and the relation to body and neck size. *Stroke* 2006; 37: 1103–1105.
44. Schrauben E, Wåhlin A, Ambarki K, et al. Fast 4D flow MRI intracranial segmentation and quantification in tortuous arteries. *J Magnet Reson Imag* 2015; 42: 1458–1464.
45. de Riva N, Budohoski KP, Smielewski P, et al. Transcranial Doppler pulsatility index: what it is and what it isn't. *Neurocrit Care* 2012; 17: 58–66.
46. Hanon O, Haulon S, Lenoir H, et al. Relationship between arterial stiffness and cognitive function in elderly subjects with complaints of memory loss. *Stroke* 2005; 36: 2193–2197.
47. Alber J, Alladi S, Bae H-J, et al. White matter hyperintensities in vascular contributions to cognitive impairment and dementia (VCID): knowledge gaps and opportunities. *Alzheimers Dement* 2019; 5: 107–117.
48. Tarbell JM, Shi Z-D, Dunn J, et al. Fluid mechanics, arterial disease, and gene expression. *Annu Rev Fluid Mech* 2014; 46: 591–614.
49. Farrall AJ and Wardlaw JM. Blood–brain barrier: ageing and microvascular disease – systematic review and meta-analysis. *Neurobiol Aging* 2009; 30: 337–352.
50. Wåhlin A and Nyberg L. At the heart of cognitive functioning in aging. *Trends Cogn Sci* 2019; 23: 717–720.
51. Geurts LJ, Zwanenburg JJM, Klijn CJM, et al. Higher pulsatility in cerebral perforating arteries in patients with small vessel disease related stroke, a 7T MRI study. *Stroke* 2019; 50: 62–68.
52. Berman SE, Clark LR, Rivera-Rivera LA, et al. Intracranial arterial 4D flow in individuals with mild cognitive impairment is associated with cognitive performance and amyloid positivity. *J Alzheimers Dis* 2017; 60: 243–252.
53. Arbel-Ornath M, Hudry E, Eikermann-Haerter K, et al. Interstitial fluid drainage is impaired in ischemic stroke and Alzheimer's disease mouse models. *Acta Neuropathol* 2013; 126: 353–364.
54. Mestre H, Kostrikov S, Mehta RI, et al. Perivascular spaces, glymphatic dysfunction, and small vessel disease. *Clin Sci* 2017; 131: 2257–2274.

55. Asgari M, de Zélicourt D and Kurtcuoglu V. Glymphatic solute transport does not require bulk flow. *Sci Rep* 2016; 6: 38635.
56. Bakker ENTP, Bacskai BJ, Arbel-Ornath M, et al. Lymphatic clearance of the brain: perivascular, paravascular and significance for neurodegenerative diseases. *Cell Mol Neurobiol* 2016; 36: 181–194.
57. Weller RO, Boche D and Nicoll JAR. Microvasculature changes and cerebral amyloid angiopathy in Alzheimer's disease and their potential impact on therapy. *Acta Neuropathol* 2009; 118: 87–102.
58. Diem AK, MacGregor Sharp M, Gatherer M, et al. Arterial pulsations cannot drive intramural periarterial drainage: significance for Aβ drainage. *Front Neurosci* 2017; 11: 475.
59. Mahley RW. Apolipoprotein E: from cardiovascular disease to neurodegenerative disorders. *J Mol Med* 2016; 94: 739–746.
60. Broce IJ, Tan CH, Fan CC, et al. Dissecting the genetic relationship between cardiovascular risk factors and Alzheimer's disease. *Acta Neuropathol* 2019; 137: 209–226.
61. Fazlollahi A, Calamante F, Liang X, et al. Increased cerebral blood flow with increased amyloid burden in the preclinical phase of Alzheimer's disease. *J Magnet Reson Imag* 2020; 51: 505–513.